Solar Energy Vol. 44, No. 5, pp. 249–256, 1990
Printed in the U.S.A.

0038-092X/90 $3.00 + .00

A SIMPLE PROCEDURE FOR CORRECTING SHADOWBAND DATA FOR ALL SKY CONDITIONS

B. A. LEBARON,* J. J. MICHALSKY,† and R. PEREZ†
*Pacific Northwest Laboratory, Richland, Washington 99352, †Atmospheric Sciences Research Center, State University of New York at Albany, Albany, NY 12205, USA

Abstract—A model is presented that corrects the horizontal diffuse irradiance measured using a polar-axis design shadowband. Ratios of true diffuse to uncorrected diffuse measurements are categorized and averaged according to parameters describing the associated geometric screening and current sky conditions. The screening parameter is a geometric calculation for the amount of the sky hemisphere eclipsed by the band. The sky condition parameters account for the anisotropic distribution of the diffuse irradiance across the sky hemisphere. An independent set of shadowband diffuse data is corrected using this parameterization technique. Comparison of these corrected values with concurrent true diffuse irradiance values gives a root mean square error of 6.9 W/m^2 and a regression slope of 0.99. The anisotropic contribution to the total shadowband correction is examined for seven different levels of sky clearness and indicates the importance of its consideration in the model's development. Since the correction ratios are developed from parameters that are not site specific, the model should be generally applicable.

1. INTRODUCTION

For solar resource assessment, the global and diffuse horizontal irradiance and the direct normal irradiance are of primary interest. They are related according to the equation

$$\mathrm{Glo}_h = \mathrm{Dif}_h + \cos(\mathrm{Zen}) * \mathrm{Dir}_n \qquad (1)$$

where Glo_h is the global horizontal irradiance, Dif_h is the diffuse horizontal irradiance, Dir_n is the direct normal irradiance, and Zen is the zenith angle of the sun. A monitoring station typically measures only two of the insolation components and calculates the third. Thus, the diffuse horizontal irradiance can either be measured or be derived from measurements of the global horizontal and direct normal irradiance. Often the diffuse component is measured and the direct calculated because of the capital and maintenance expense associated with solar tracking for the direct normal measurement.

Measuring the diffuse component requires that the detector be shaded from the direct sun by an occulting device. Tracking shadow disks are sometimes employed, but they have fiscal drawbacks similar to those associated with measuring the direct normal insolation. More often a fixed shadowband is used to shade the detector from sunrise to sunset. In its most common form the shadowband uses a polar axis design[1] requiring adjustment for solar declination every few days. A correction must be applied to the measured diffuse irradiance, however, since the band also blocks a portion of the sky hemisphere. The accuracy of this correction is important since any subsequent calculation of the direct component is affected, particularly for high zenith angles. For example, from eqn (1), a 5% error in the horizontal diffuse irradiance measurement will propagate to more than 20% for the calculated direct normal irradiance at zenith angles greater than 75 degrees.

Methods that correct for the shadowband's presence assuming the diffuse irradiance is isotropically distributed are available for various geometric configurations[2–4]. Drummond[2] derived a formula that can be applied worldwide to estimate the amount of diffuse irradiance blocked by a shadowband having polar geometry. It is a geometrical calculation for the fraction of the sky hemisphere that is obscured by the shadowband as viewed by the detector. The diffuse measurement is then increased by this fraction with the assumption that the distribution of sky radiation is isotropic. Applying this geometric correction to a large amount of data from South Africa, Drummond showed that on average it underestimated the diffuse component for clear and overcast periods by 7% and 3%, respectively[5]. He attributed this deficit to the anisotropic distribution of the diffuse irradiance, which tends to be weakest on overcast days and strongest on turbid days when atmospheric aerosols cause broadening of the circumsolar region. Further, his examination indicated that for clear sky, this additional amount was seasonally dependent but did not appear to be a function of zenith angle.

Several investigators have stressed the importance of the anisotropic contribution to the total shadowband correction. Under near-cloudless conditions at the Dead Sea, Stanhill[6] found that anisotropic sky corrections ranged between 14% and 30% above the geometric correction calculated for different times of the year. He also noted that the variations in the correction were correlated with synoptic weather patterns and surmised that they resulted from changes in the strength of the circumsolar component caused by the intruding aerosol burden and size distribution. Painter[7] investigated the deficiencies of applying only the isotropic,

Portions of this paper were presented at the American Solar Energy Society Meeting in Denver, 1989.

geometric correction to diffuse insolation measurements made by the United Kingdom Meteorological Office. He developed functions based on declination and clearness (the ratio of diffuse-to-global irradiance) that could be applied to estimate the additional anisotropic correction. For his comparisons near Bracknel, England, values ranged between less than 1% and 14%.

Steven[8] used a two parameter model to describe the relationship between an isotropic background component and a circumsolar component for sky conditions from clear to overcast. The ratio of diffuse-to-global irradiance was used to define the fraction of possible sunshine and in turn the parameter values. However, as the author noted, the diffuse-to-global ratio is affected by a variety of physical conditions and other parameterizations may be more appropriate for characterizing the sky anisotropy.

An empirical model developed by Kasten[9] and applied by others[10,11] used cloudiness, turbidity, and declination parameters to characterize the sky conditions. Multivariate-linear regression was used to derive an equation containing these terms that could estimate the anisotropic correction. While applications of the model suggested good agreement with true diffuse values for the site where it was derived, attempts to transfer the function to other sites and other band types were less than satisfactory[10]. This weakness represents a significant drawback because it means that initially a large amount of site-specific data (six months between winter and summer solstices) will be required to generate an appropriate correction equation.

An additional source of error in the diffuse irradiance measurement can be introduced because of reflection from the band's interior surface onto the detector. This contribution is strongest at high solar zenith angles near the summer and winter solstices. The effect of shadowband reflection was examined in detail by LeBaron *et al.*[12] for shadowbands having an albedo greater than zero.

The amount of diffuse irradiance blocked by a shadowband at any given time is a function of both the geometric portion of the sky hemisphere that is screened (a straightforward calculation) and the prevailing sky conditions, which dictate how the diffuse irradiance is distributed. Reflection from the bands interior at high solar-zenith angles can also have an effect. These factors are related by

$$C_t = C_i C_a C_r \tag{2}$$

where C_t is the total shadowband correction ratio of true to uncorrected diffuse, C_i is the isotropic shadowband correction factor, C_a is the anisotropic shadowband correction factor and, C_r is the shadowband reflection factor.

Calculating the geometric fraction of the sky screened (C_i) has been adequately addressed by Drummond[2] for the case of the polar-axial shadowband geometry, as stated previously. However, the additional amount of correction that may be required because of the existing sky conditions (C_a) is not a simple analytical calculation in real atmospheres and must be based on experimental information. The effect of reflection on the correction is considered minimal because, typically, shadowbands are painted with a low albedo black.

In this paper we use a parameterization scheme to define a set of correction factors covering unique combinations of sky and geometric screening conditions. This scheme relies on the method of Perez *et al.*[13] for characterizing sky anisotropy which has been satisfactorily validated for many sites worldwide. Since we have defined our corrections without regard to site-specific factors, the model should be applicable for other geographic locations.

2. PARAMETERIZATION METHOD

The correction model uses four parameters to describe both the isotropic (geometric) and anisotropic (sky condition) effects. Thus, the factor derived is the total correction of the shadowband diffuse irradiance measurement needed to obtain the true diffuse value.

Three parameters are used to describe the anisotropic contribution to the total shadowband correction. We follow the scheme developed by Perez *et al.*[14], who have successfully used a similar parameterization technique to characterize the anisotropic nature of skylight in modeling irradiance on an arbitrarily oriented surface. The zenith angle is used as a parameter to index the position of the sun in the vertical plane. Epsilon and delta are parameters that index the sky's clearness and brightness, respectively, the clearness index being primarily a function of the cloud condition and the brightness index a function of the cloud thickness or aerosol loading. Here, epsilon is a simplification of the term used by Perez *et al.*[14] in that it is not corrected for solar zenith angle. If we define

$$\mathrm{Dir}_{nu} = (\mathrm{Glo}_h - \mathrm{Dif}_{hu})/\cos(\mathrm{Zen}),$$

then

$$\mathrm{epsilon} = (\mathrm{Dif}_{hu} + \mathrm{Dir}_{nu})/\mathrm{Dif}_{hu},$$

and

$$\mathrm{delta} = \mathrm{Dif}_{hu} * am/I_0.$$

Dir_{nu} and Dif_{hu} are the uncorrected direct normal and diffuse horizontal irradiances, Glo_h is the global horizontal irradiance, I_0 is the extraterrestrial irradiance, am is the air mass, and Zen is the zenith angle of the sun. Note that the parameters epsilon and delta are based only on measurements of the global and uncorrected diffuse irradiance.

The fourth parameter is an isotropic calculation for the fraction of the sky hemisphere that is screened by a polar axial design shadowband. It is defined as follows:

$$X/T = [2b/\pi r]\cos^3\delta(\sin\phi t_0 + \cos\phi\cos\delta\sin t_0)$$

where r is the radius of the shadowband, b is the width of the shadowband, t_0 is the sunset/sunrise hour angle, ϕ is the latitude, and δ is the declination. The derivation of this equation is described in detail by Drummond[2].

Using these four parameters, a variety of states can be identified which, in turn, dictate the factor needed to correct the diffuse irradiance measured under the shadowband. Given that a variety of data is used in the model development to cover all possible states, and given that the parameterization has been shown to be site-independent, the model should be generally applicable.

3. DATA SET AND ANALYSIS

We used two years of data from Albany, New York, and from Bluefield, West Virginia, to develop our parameterization model. The data consist of hourly values of measured global and diffuse horizontal irradiance and direct normal irradiance. The two sites provide some variation in climatic conditions and latitude separation, lending diversification to the model.

As part of the archiving procedures, each site incorporated its own quality control flags into the data, identifying tracking error for the direct normal irradiance measurement, shadowband misalignment, and other questionable data. This information was applied where possible to cull the data set, to increase reliability. In total, 3786 hours of data from the Bluefield site and 4563 hours of data from the Albany site were used in the model development and verification.

Several analytical checks for instrument calibration were performed. The instruments at the Albany site were consistent; however, the Bluefield instrument measuring global horizontal irradiance was found to be low by 2.56%, and the data values were adjusted accordingly.

The four parameters—solar zenith angle, geometric screening, epsilon, and delta—were calculated for each hour of data. The hourly values of true diffuse irradiance were calculated from the measured values of global horizontal and direct normal irradiance according to eqn (1). Two-thirds of the data were used to develop the model, with the remaining third (every third hourly record) reserved for validation.

The corrections were developed by grouping hourly data according to the parameter boundaries listed in Table 1. Each parameter was separated into four divisions, creating a model having 256 unique categories or descriptions of geometric and sky conditions. For each category a mean ratio of true diffuse to uncorrected diffuse (Dif_h/Dif_{hu}) was calculated. Note that what may appear as an over determination of 256 terms represents in effect a "digitization" of a more complex analytical formulation. For computer applications, a 256-element array look-up is considerably more efficient than analytical computations.

Table 2 provides a way of looking up the mean correction ratio for a particular category. The indices of the four-way table are, in order, solar zenith angle, geometric screening, epsilon, and delta. For example, the index (3,4,1,3) would describe a state having a 50- to 60-degree solar zenith angle, greater than 13.2% geometric screening, overcast skies, and average to high sky brightness. According to the model, this category has a correction ratio of 1.129, meaning the measured diffuse irradiance would need to be increased by 12.9% to equal the true diffuse irradiance. Some categories are not defined either because of the physical range limits of the current data set or because of unphysical combinations of parameters. For these categories (underlined in Table 2) we used the mean geometric correction based on Drummond's formula. The model is applied to uncorrected diffuse measurements by simply classifying the prevailing conditions according to the four parameters and correcting the value by the mean ratio for the corresponding category.

Table 1. Boundaries used for the four parameters chosen to describe the anisotropic shadowband correction. The resulting four-way table has 256 categories

Cuts	1	2	3	4	
Zenith	0.000	35.00	50.00	60.00	90.00
Geometric	1.000	1.068	1.100	1.132	—
Epsilon	0.000	1.253	2.134	5.980	—
Delta	0.000	0.120	0.200	0.300	—

An examination of Table 2 reveals that the shadowband correction factor ranges from 0.935 to 1.248. The highest values occur when the geometric screening is high, there are few clouds, and the sky brightness is high. This state is typical of high solar declination, when a large portion of the shadowband is above the horizon and clear, hazy sky conditions exist. Smaller correction values are evident for the overcast sky condition, when the clearness index is equal to one, as one would expect. However, interestingly, the lowest correction values (in some cases less than one) occur when the sky is very clear, the geometric screening is low, and zenith angle is high. These low values may be the result of reflection from the shadowband's interior back to the detector, or the cosine response of the global horizontal detector artificially degrading the calculation of the true diffuse irradiance.

Table 2 also indicates a clear pattern of decreasing correction ratio with increasing solar zenith angle. This finding is in conflict with other investigations that find no zenith angle dependence[2,7,11]. However, zenith angle dependence should be expected if one investigates the principal cause of the decrease: the solar aureole contribution. For a given geometric correction and aureole brightness, the difference between uncorrected and true diffuse due to aureole scattering should decrease linearly with the cosine of the solar-zenith angle. Band reflection would also tend to reduce the correction ratio.

4. VALIDATION

Scatter plots of the true diffuse irradiance (calculated from measurements of the global horizontal and direct normal irradiance using eqn (1)) vs. the uncorrected

Table 2. Shadowband correction ratios for each of the parameterized catagories
(i = zenith; j = geometric; k = epsilon, l = delta)

(i,j,1,1)

i=	j=(,1)	(,2)	(,3)	(,4)
(1,)	1.051	1.082	1.117	1.173
(2,)	1.051	1.104	1.115	1.163
(3,)	1.069	1.082	1.119	1.140
(4,)	1.047	1.063	1.074	1.030

(i,j,2,1)

i=	j=(,1)	(,2)	(,3)	(,4)
(1,)	1.051	1.082	1.117	1.248
(2,)	1.051	1.082	1.117	1.184
(3,)	1.161	1.161	1.147	1.168
(4,)	1.076	1.078	1.104	1.146

(i,j,3,1)

i=	j=(,1)	(,2)	(,3)	(,4)
(1,)	1.051	1.082	1.117	1.156
(2,)	1.051	1.082	1.117	1.156
(3,)	1.051	1.082	1.117	1.156
(4,)	1.187	1.167	1.139	1.191

(i,j,4,1)

i=	j=(,1)	(,2)	(,3)	(,4)
(1,)	1.051	1.082	1.117	1.181
(2,)	1.051	1.082	0.990	1.104
(3,)	1.015	1.016	0.946	1.027
(4,)	0.925	0.967	0.977	1.150

(i,j,1,2)

i=	j=(,1)	(,2)	(,3)	(,4)
(1,)	1.051	1.082	1.117	1.176
(2,)	1.051	1.095	1.130	1.162
(3,)	1.073	1.089	1.115	1.142
(4,)	1.058	1.076	1.117	1.156

(i,j,2,2)

i=	j=(,1)	(,2)	(,3)	(,4)
(1,)	1.051	1.082	1.117	1.211
(2,)	1.051	1.082	1.186	1.194
(3,)	1.086	1.130	1.168	1.177
(4,)	1.074	1.102	1.118	1.174

(i,j,3,2)

i=	j=(,1)	(,2)	(,3)	(,4)
(1,)	1.051	1.082	1.117	1.237
(2,)	1.051	1.082	1.203	1.212
(3,)	1.080	1.195	1.211	1.185
(4,)	1.140	1.098	1.191	1.181

(i,j,4,2)

i=	j=(,1)	(,2)	(,3)	(,4)
(1,)	1.051	1.082	1.117	1.217
(2,)	1.051	1.082	1.120	1.180
(3,)	1.182	1.115	1.081	1.111
(4,)	1.057	1.119	1.133	1.033

(i,j,1,3)

i=	j=(,1)	(,2)	(,3)	(,4)
(1,)	1.051	1.082	1.117	1.182
(2,)	1.051	1.082	1.128	1.159
(3,)	1.076	1.088	1.131	1.129
(4,)	1.060	1.085	1.103	1.156

(i,j,2,3)

i=	j=(,1)	(,2)	(,3)	(,4)
(1,)	1.051	1.082	1.117	1.221
(2,)	1.051	1.171	1.180	1.213
(3,)	1.135	1.148	1.176	1.197
(4,)	1.092	1.119	1.143	1.182

(i,j,3,3)

i=	j=(,1)	(,2)	(,3)	(,4)
(1,)	1.051	1.082	1.117	1.238
(2,)	1.051	1.160	1.207	1.230
(3,)	1.169	1.191	1.193	1.210
(4,)	1.150	1.133	1.180	1.156

(i,j,4,3)

i=	j=(,1)	(,2)	(,3)	(,4)
(1,)	1.051	1.082	1.117	1.156
(2,)	1.051	1.082	1.117	1.156
(3,)	1.051	1.082	1.117	1.156
(4,)	1.089	1.194	1.216	1.064

(i,j,1,4)

i=	j=(,1)	(,2)	(,3)	(,4)
(1,)	1.051	1.082	1.117	1.191
(2,)	1.051	1.105	1.143	1.168
(3,)	1.085	1.093	1.117	1.156
(4,)	1.069	1.082	1.117	1.156

(i,j,2,4)

i=	j=(,1)	(,2)	(,3)	(,4)
(1,)	1.051	1.082	1.117	1.238
(2,)	1.051	1.148	1.195	1.230
(3,)	1.132	1.160	1.183	1.210
(4,)	1.118	1.116	1.150	1.185

(i,j,3,4)

i=	j=(,1)	(,2)	(,3)	(,4)
(1,)	1.051	1.082	1.117	1.232
(2,)	1.051	1.206	1.210	1.238
(3,)	1.144	1.178	1.226	1.216
(4,)	1.117	1.155	1.178	1.167

(i,j,4,4)

i=	j=(,1)	(,2)	(,3)	(,4)
(1,)	1.051	1.082	1.117	1.156
(2,)	1.051	1.082	1.117	1.156
(3,)	1.051	1.082	1.117	1.156
(4,)	1.024	1.025	1.162	1.142

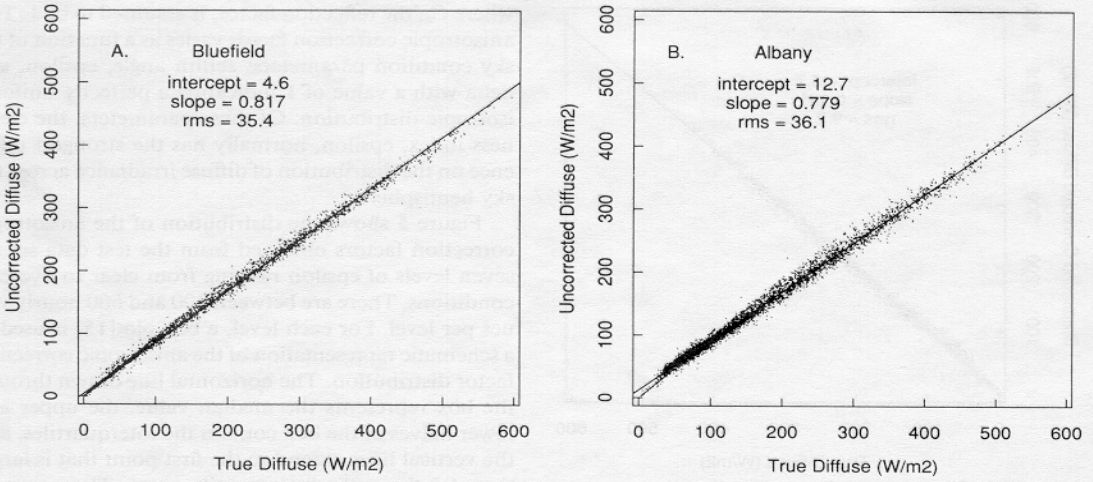

Fig. 1. Scatter plots showing the relationship between true diffuse irradiance calculated from eqn (1) and uncorrected shadowband diffuse irradiance for the two data sets. The line represents a least squares fit to the points.

diffuse irradiance for both Bluefield and Albany are shown in Fig. 1. The regression statistics are given, and a line representing the best fit is drawn through the points. A linear fit is used only to generally characterize the points. The relationship is actually somewhat curved, being a function of the four parameters discussed above. Note that the general slope of the data for the two sites differs by a few percent because of differences in latitude, average sky anisotropy, and temporal data distribution. The root mean square (rms) error is based on departures of measured diffuse from calculated (true) diffuse. It is clear from the size of this error that failure to correct for the band's presence will lead to very large measurement errors (approx. 35 W/m^2 for each of the data sets).

Our parameterization model was applied to the test data set (one third of the data from both sites) and the results regressed against the true diffuse irradiance to determine the model performance. The results of this comparison are shown in Fig. 2. along with the regression statistics. The rms error has been reduced to 6.9 W/m^2, and the slope is nearly one.

The results of applying Drummond's isotropic shadowband correction to the test data set were also examined. Applying only the geometric correction for the portion of the sky hemisphere screened by the shadowband underestimates the true diffuse irradiance, as is widely known. For our test data set the rms error is 13.4 W/m^2 with a slope of 0.924. Subsequently, we increased the geometric correction an additional 4%, as suggested by Drummond[5] to relate isotropic to average real sky conditions (Fig. 3.). The rms error is still 34% greater than for the parameterization model, and the slope is significantly less than one. A careful examination of the figure shows that curvature remains in the relationship, an indication of the variation in the anisotropic parameters, solar zenith angle, epsilon, and delta.

In Fig. 4. we show a five-day time series of hourly diffuse data measured with a shadowband. The points represent the calculated true diffuse values, the crosses are the measured diffuse corrected using the parameterization model, and the circles represent the measured diffuse corrected using the geometric factor (C_i). Both correction methods work equally well on days when the sky anisotropy is not great. For example, under overcast conditions (day 178) the parameterization correction offers little improvement over the isotropic correction. The parameterization correction is somewhat more accurate on clear days at low solar zenith angles (day 179), though it still tends toward over prediction. However, under partially cloudy sky conditions

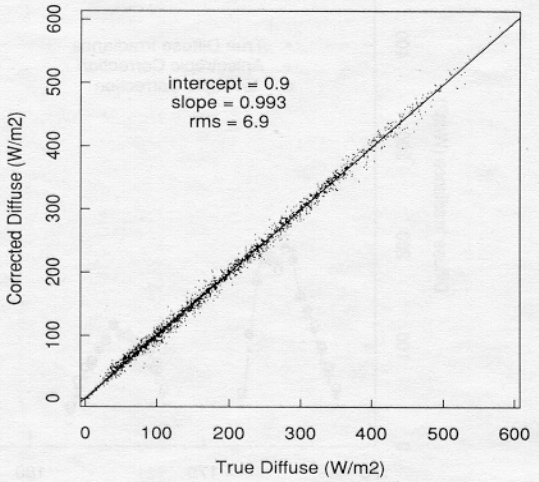

Fig. 2. Scatter plot of true diffuse irradiance (eqn (1)) vs. shadowband diffuse irradiance corrected using the parameterization model. The line represents a least squares fit to the points.

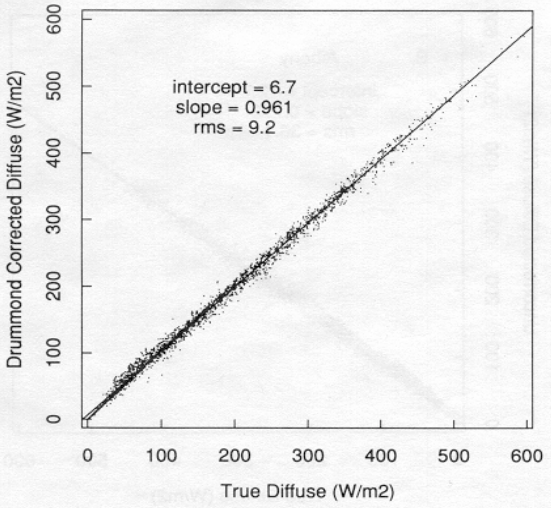

Fig. 3. Scatter plot of true diffuse irradiance (eqn (1)) and shadowband diffuse irradiance corrected using Drummond's geometric formula. An additional 4% was included for average sky anisotropy.

that produce the highest diffuse irradiance values and represent the most anisotropic distributions, the parameterization model provides a significantly better correction.

5. THE ANISOTROPIC CONTRIBUTION

It is possible to identify the anisotropic portion (C_a) of the total shadowband correction (C_t) from eqn (2) by taking the ratio:

$$C_a = C_t/C_i$$

where C_r, the reflection factor, is assumed to be 1. This anisotropic correction factor varies as a function of the sky condition parameters; zenith angle, epsilon, and delta with a value of 1 indicating a perfectly uniform isotropic distribution. Of these parameters, the clearness index, epsilon, normally has the strongest influence on the distribution of diffuse irradiance across the sky hemisphere.

Figure 5 shows the distribution of the anisotropic correction factors obtained from the test data set for seven levels of epsilon ranging from clear to overcast conditions. There are between 200 and 600 hourly values per level. For each level, a box plot[15] is used as a schematic representation of the anisotropic correction factor distribution. The horizontal line drawn through the box represents the median value, the upper and lower halves of the box contain the interquartiles, and the vertical lines extend to the first point that is larger than 1.5 times the interquartile range. The nonoverlapping of the box notches indicate a significant difference at roughly the 5% level.

The most important feature of Fig. 5. is the change in the median amount of anisotropy with clearness. For overcast skies (epsilon = 1.0–1.2) the anisotropic correction factor is very close to unity as would be expected since diffuse irradiance tends to be more uniformly distributed under these conditions. As clearness increases, the median anisotropic correction factor also steadily increases until a fairly high level of clearness is reached. For higher levels of epsilon the anisotropy begins to decline. This decline is because of the increasing influence of the clear sky background which tends to be darker in the zenith direction. For the clearest skies, the anisotropy drops off sharply to a median value less than one. The implication is that the

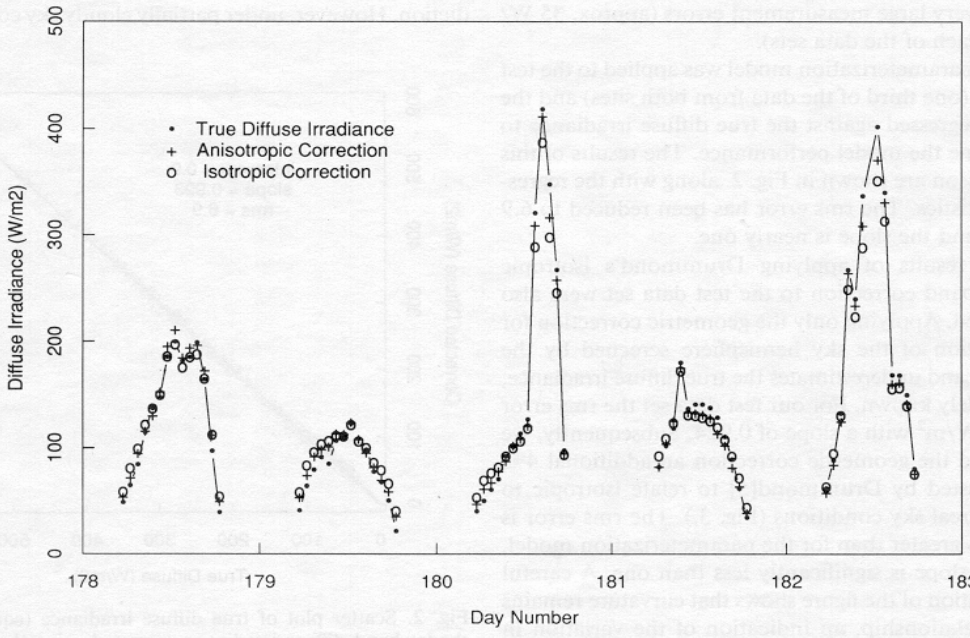

Fig. 4. Five-day time series of hourly diffuse irradiance showing a comparison between true diffuse and shadowband diffuse corrected using an isotropic model and our anisotropic model.

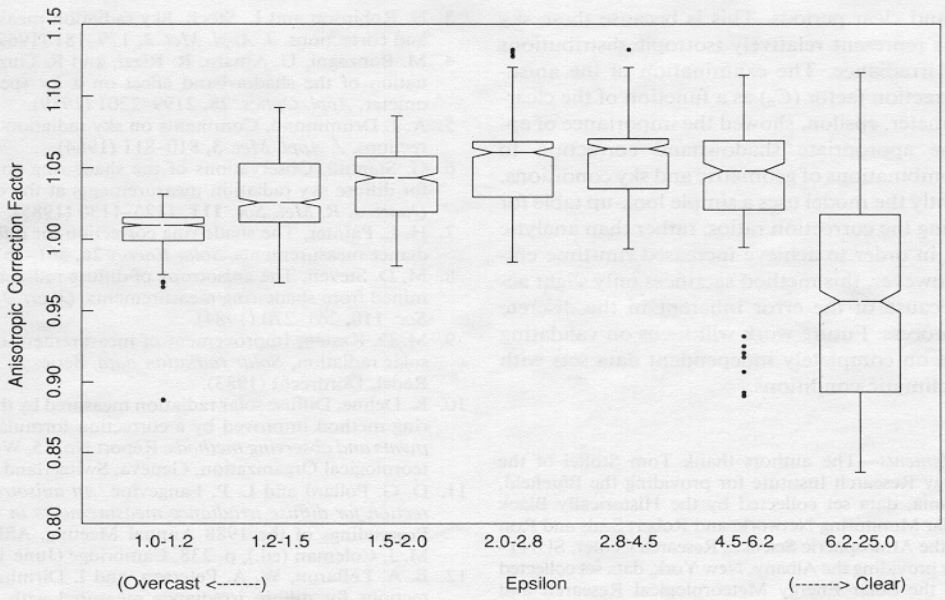

Fig. 5. Box plots representing the distribution of the anisotropic correction factor for seven levels of the clearness parameter, epsilon.

geometric correction factor (C_i) must be reduced to arrive at the true diffuse irradiance.

The range in the anisotropic correction factor values for the various clearness levels suggests the following: overcast skies are nearly isotropic (although values slightly in excess of one indicate the characteristic zenith brightening of these skies) with little variation, partially clear skies are strongly anisotropic but have greater variance, and the clearest skies exhibit a darker zenith than horizon allowing anisotropic values less than unity.

This qualitative examination of the dependence of anisotropy on only one of our model (though probably the most influential) parameters, epsilon, shows the potential error that can result from simply applying a constant value (e.g., Drummond's 4%) to relate isotropic to real sky conditions.

While a constant value may be adequate for correcting long-term average irradiance values, individual diffuse measurements corrected in this fashion will have errors approaching 10%. This is a significant problem if the corrected diffuse measurement will be used in conjunction with a global measurement to derive the direct irradiance component according to eqn (1).

6. CONCLUSIONS

We have described a model that utilizes four parameters to account for both the isotropic and anisotropic contributions to the total shadowband correction ratio. The parameterization scheme provides the flexibility to identify a wide range of anisotropic states. This flexibility makes the model generally applicable, limited only by the data used to fill the look-up table. The model's general transferability is further ensured by the wide validation of this anisotropic parameterization in previous radiation models.

Based on measured data from two independent sites, the true diffuse (calculated from global horizontal and direct normal irradiance) is ratioed to the uncorrected horizontal diffuse measurement to determine appropriate correction ratios for unique combinations of geometric and sky condition parameters. The highest correction ratios occur during conditions of substantial geometric screening by the shadowband, clear sky, and large aerosol optical depth. Small correction ratios, a few percent above one, are found for low declination (little geometric screening), overcast, thick cloud layer conditions. Conditions of clear sky and low aerosol loading provide the smallest corrections, in some cases less than one for high solar zenith angles. This result may be caused primarily by direct reflection from the band's interior or the cosine response of the global horizontal irradiance detector used to calculate true diffuse.

Validation with an independent data set shows that our anisotropic model, based only on measurements of the global horizontal and uncorrected diffuse horizontal irradiance, provides a reliable correction for the two measurement sites. The model performs significantly better than the widely used geometric correction derived by Drummond even when an additional 4% is included to account for anisotropy.

It is for the strongly anisotropic conditions of partially clear skies, when the diffuse irradiance tends to be high, that our parameterization scheme can make a significant improvement over the Drummond formula. Less accuracy improvement is realized for the

overcast and clear periods. This is because these sky conditions represent relatively isotropic distributions of diffuse irradiance. The examination of the anisotropic correction factor (C_a) as a function of the clearness parameter, epsilon, showed the importance of applying the appropriate shadowband correction to unique combinations of geometric and sky conditions.

Currently the model uses a simple look-up table for determining the correction ratios, rather than analytic formulas, in order to achieve increased run-time efficiency. However, this method sacrifices only slight accuracy because of the error inherent in the discrete binning process. Future work will focus on validating the model on completely independent data sets with different climatic conditions.

Acknowledgments—The authors thank Tom Stoffel of the Solar Energy Research Institute for providing the Bluefield, West Virginia, data set collected by the Historically Black College Solar Monitoring Network, and Robert Seals and Ron Stewart of the Atmospheric Sciences Research Center, SUNY-Albany, for providing the Albany, New York, data set collected as part of the Solar Energy Meteorological Research and Training Site Program. This work was supported by the Office of Basic Energy Sciences within the U.S. Department of Energy under Contract DE-AC06-76RLO 1830.

REFERENCES

1. K. L. Coulson, *Solar and terrestrial radiation, methods and measurements,* Academic Press, New York (1975).
2. A. J. Drummond, On the measurement of sky radiation, *Arch. Meteor. Geophys. Bioklim.* **7,** 413–436 (1956).
3. N. Robinson and L. Stoch, Sky radiation measurement and corrections, *J. Appl. Met.* **3,** 179–181 (1969).
4. M. Bonzagni, U. Amato, R. Rizzi, and R. Guzzi, Evaluation of the shadowband effect on a 2π spectroradiometer, *Appl. Optics.* **28,** 2199–2201 (1989).
5. A. J. Drummond, Comments on sky radiation and corrections, *J. Appl. Met.* **3,** 810–811 (1964).
6. G. Stanhill, Observations of the shade-ring corrections for diffuse sky radiation measurements at the dead sea, *Quart. J. R. Met. Soc.* **111,** 1125–1130 (1985).
7. H. E. Painter, The shade ring correction for diffuse irradiance measurements, *Solar Energy* **26,** 361–363 (1981).
8. M. D. Steven, The anisotropy of diffuse radiation determined from shade-ring measurements, *Quart. J. R. Met. Soc.* **110,** 261–270 (1984).
9. M. D. Kasten, Improvement of measurement of diffuse solar radiation, *Solar radiation data,* Series F, 2 ed. D. Redel, Dordrecht (1983).
10. K. Dehne, Diffuse solar radiation measured by the shade-ring method improved by a correction formula, *Instruments and observing methods,* Report No. 15, World Meteorological Organization, Geneva, Switzerland (1984).
11. D. G. Pollard and L. P. Langevine, *An anisotropic correction for diffuse irradiance measurements in Guyana,* Proceedings of the 1988 Annual Meeting, ASES, Inc., M. J. Coleman (ed.), p. 238, Cambridge (June 1988).
12. B. A. LeBaron, W. A. Peterson, and I. Dirmhirn, Corrections for diffuse irradiance measured with shadowbands, *Solar Energy* **25,** 1–13 (1980).
13. R. Perez, R. Seals, P. Ineichen, R. Stewart, and D. Menicucci, A new simplified version of the Perez diffuse irradiance model for tilted surfaces, *Solar Energy* **39,** 221–231 (1987).
14. R. Perez, P. Ineichen, R. Seals, J. Michalsky, and R. Stewart, Models that use global and direct irradiance input to predict other irradiance and daylight availability quantities. *Solar Energy* (in press).
15. J. M. Chambers, W. S. Cleveland, B. Kleiner, and P. A. Tukey, *Graphical methods for data analysis,* Wadsworth, International Group, California (1983).